

# Riccati-ZORO: An efficient algorithm for heuristic online optimization of internal feedback laws in robust and stochastic model predictive control

Florian Messerer<sup>1</sup>, Yunfan Gao<sup>1</sup>, Jonathan Frey<sup>1</sup>, Moritz Diehl<sup>1,2</sup>

**Abstract**—We present Riccati-ZORO, an algorithm for tube-based optimal control problems (OCP). Tube OCPs predict a tube of trajectories in order to capture predictive uncertainty. The tube induces a constraint tightening via additional backoff terms. This backoff can significantly affect the performance, and thus implicitly defines a cost of uncertainty. Optimizing the feedback law used to predict the tube can significantly reduce the backoffs, but its online computation is challenging.

Riccati-ZORO jointly optimizes the nominal trajectory and uncertainty tube based on a heuristic uncertainty cost design. The algorithm alternates between two subproblems: (i) a nominal OCP with fixed backoffs, (ii) an unconstrained tube OCP, which optimizes the feedback gains for a fixed nominal trajectory. For the tube optimization, we propose a cost function informed by the proximity of the nominal trajectory to constraints, prioritizing reduction of the corresponding backoffs. These ideas are developed for ellipsoidal tubes under linear state feedback. In this case, the decomposition into the two subproblems yields a substantial reduction of the computational complexity with respect to the state dimension from  $\mathcal{O}(n_x^6)$  to  $\mathcal{O}(n_x^3)$ , i.e., the complexity of a nominal OCP.

We investigate the algorithm in numerical experiments, and provide two open-source implementations: a prototyping version in CasADi and a high-performance implementation integrated into the acados OCP solver.

## I. INTRODUCTION

Uncertainty-aware model predictive control (MPC), such as stochastic or robust MPC aims for an explicit treatment of predictive uncertainty [1], [2]. Typically, the main motivation is to robustify the constraints against a given model of uncertainty.

Existing approaches can be divided into two main families: Scenario- or tree-based methods represent uncertainty discretely [3], [4], [5], whereas tube-based methods use continuous uncertainty models [6], [7], [8], [9]. In tube-based methods, the uncertainty tube is typically predicted under the assumption of a simple feedback law, which mitigates the unrealistically large tubes resulting from an open-loop prediction. In general, this feedback law is only used for the uncertainty prediction within the MPC problem. The actually applied feedback is determined by the MPC policy.

In order to ease the online computational burden, this internal feedback law is typically predesigned offline. However, this comes at a loss of performance compared to online optimization, which enables the optimal manipulation of the uncertainty tube for the currently planned trajectory [10],

[11], [12]. Furthermore, and especially for nonlinear systems, it is often unclear how to predesign a simple feedback law that performs adequately over all relevant state space regions.

### A. Problem structure

In this paper, we consider tube-based optimal control problems (OCP) of the form [10], [11], [13], [14], [15]

$$\min_{x, u, K, P} \sum_{k=0}^{N-1} l_k(x_k, u_k) + l_N(x_N) \quad (1a)$$

s. t.

$$x_0 = \bar{x}_0, \quad P_0 = \bar{P}_0, \quad (1b)$$

$$x_{k+1} = f_k(x_k, u_k), \quad k = 0, \dots, N-1, \quad (1c)$$

$$P_{k+1} = \psi_k(P_k, K_k, x_k, u_k), \quad k = 0, \dots, N-1, \quad (1d)$$

$$0 \geq h_k(x_k, u_k) + b_k(P_k, K_k, x_k, u_k), \quad k = 0, \dots, N-1, \quad (1e)$$

$$0 \geq h_N(x_N) + b_N(P_N, x_N). \quad (1f)$$

Here,  $x = (x_0, \dots, x_N)$  and  $u = (u_0, \dots, u_{N-1})$  denote the nominal state and input trajectories, with nonlinear dynamics  $f_k$ . The uncertainty tube around the nominal trajectory is parametrized by  $P = (P_0, \dots, P_N)$ , and propagated under a feedback policy parametrized by  $K = (K_0, \dots, K_{N-1})$ . In this paper, we focus on the case where  $P_k$  parametrizes an ellipsoidal tube, and  $K_k$  linear state feedback.

The uncertainty tube induces a backoff  $b_k$  by which the nonlinear constraints  $h_k$  on the nominal trajectory need to be tightened in order to stay safe. This implicitly defines a cost of uncertainty via the impact of the constraint backoffs on the nominal trajectory.

Crucially, (1) optimizes the feedback parameters  $K_k$ , such that it optimally handles uncertainty for the given tube and policy parametrization. However, this is challenging to solve, both with respect to the computational cost and algorithmic robustness.

### B. Related work

Problems of structure (1) appear in robust and stochastic MPC for different tube and feedback parametrizations. In this paper, we focus on the case of ellipsoidal tubes under linear state feedback, which are propagated based on a linearization at the nonlinear nominal trajectory [10], [11], [14], [15], [16], [17]. Linearization-based propagation incurs a linearization error, which may be conservatively overbounded [13], [18], [19], [20]. The tube propagation can also be combined with learned uncertainty models such as Gaussian Processes (GP) [18], [21]. While state feedback assumes an exact measurement of

<sup>1</sup> Department of Microsystems Engineering (IMTEK), University of Freiburg, Freiburg, Germany

<sup>2</sup> Department of Mathematics, University of Freiburg, Freiburg, Germany

This research was supported by DFG via projects 424107692, 504452366 (SPP 2364) and 525018088, and by BMWK via 03EN3054B.

the state at each time step, there are also extensions to the setting of output feedback [22], [23].

The optimization over state feedback in (1) is highly nonlinear, which poses a challenge for general purpose solvers. In [24], it is shown that linear feedback over all past states can be equivalently reformulated as linear disturbance feedback. In contrast to state feedback, the optimization over disturbance feedback yields convex problems (for linear dynamics and convex costs and constraints). However, this results in  $\mathcal{O}(N^2)$  optimization variables, compared to  $\mathcal{O}(N)$  for standard state feedback. In [25], a disturbance feedback formulation is derived for the nonlinear case, with linearization-based disturbance propagation and error bounds.

Several algorithms exploit the specific structure of (1). For the case of ellipsoidal tubes, this results in a reduction of complexity per iteration from  $\mathcal{O}(n_x^6)$  to  $\mathcal{O}(n_x^3)$ , compared to using a standard OCP solver. In [26], ZORO (zero-order robust optimization) is proposed for the case of predesigned feedback gains. As a zero-order method, ZORO converges in general to a feasible point in the neighborhood of an exact solution [26]. Convergence to the exact solution can be recovered via an appropriate gradient correction [27]. A high-performance implementation of ZORO in acados [28] is presented in [29]. Real-time feasibility of ZORO for collision avoidance in mobile robotics has been demonstrated in real-world experiments [30]. An extension of ZORO to GP-based MPC is presented in [31], with an efficient implementation in [32] extending the acados ZORO implementation. In [33], ZORO is adapted for time-optimal motion planning.

SIRO (Sequential inexact robust optimization) [11] solves (1) exactly, for the case that the tube follows Lyapunov dynamics under linear state feedback. In this case, the optimality conditions of (1) define the optimal feedback gains as the solution of a linear quadratic regulator (LQR) problem, in which the uncertainty in the constraint directions is weighted by the corresponding Lagrange multipliers. Local convergence of SIRO is proven in [11] under the assumption of a stable active set. However, subsequent experiments have revealed that for some practically relevant problems this assumption is not always fulfilled. SIRO is extended to linear disturbance feedback in [34], and adapted for time-optimal motion planning in [15].

Furthermore, several algorithms perform heuristic online optimization of the feedback gains. The algorithm in [13] can be seen as a modification of ZORO, updating the feedback gains in each iteration by solving an LQR problem. The authors in [14] use the sensitivities of the nominal OCP solution as an approximation of future MPC feedback. In [20], a semidefinite program (SDP) is solved to jointly update the tube and feedback gain parameters for the current nominal trajectory.

### C. Contribution and Outline

In this paper, we propose the algorithm Riccati-ZORO for the heuristic optimization of feedback gains in (1). This generalizes ZORO [26], [29], which addresses (1) for the case of predesigned feedback. As in [13], Riccati-ZORO

optimizes the feedback gains in each iteration with respect to a heuristically designed cost related to LQR. In contrast to the constant cost weights in [13], we update the weights based on constraint proximity in order to mimic the effect of exact feedback gain optimization. From this perspective, Riccati-ZORO is a heuristic variation of SIRO [11], giving the user more control over the tube shaping subproblem.

Riccati-ZORO is made available via two open-source implementations: (i) a prototyping version in CasADi [35], (ii) a high-performance implementation in acados [28], extending the ZORO implementation [29].

This paper is structured as follows. Section II introduces the treated ellipsoidal tube OCP, and Section III revisits the LQR from a tube perspective. Section IV defines the proposed algorithm and cost design, with a brief discussion of optimality and convergence in Section V. Section VI describes the implementation in acados, followed by numerical experiments in Section VII and a concluding Section VIII.

### D. Notation and preliminaries

For vectors  $x \in \mathbb{R}^n$ ,  $y \in \mathbb{R}^m$  we denote by  $(x, y) := [x^\top, y^\top]^\top$  their vertical concatenation. For a vector-valued function  $f: \mathbb{R}^n \rightarrow \mathbb{R}^q$ , we denote by  $\nabla f(x) \in \mathbb{R}^{n \times q}$  the gradient, which is the transpose of the Jacobian  $\frac{\partial f(x)}{\partial x}$ . For a function with multiple arguments,  $g: \mathbb{R}^n \times \mathbb{R}^m \rightarrow \mathbb{R}^q$ , we use  $\nabla g(x, y)$  to denote the vertically concatenated gradient w.r.t. both arguments, or specify the argument as  $\nabla_x g(x, y)$ . Each symmetric positive semidefinite matrix  $Q \in \mathbb{S}_+^n$  defines an ellipsoid  $\mathcal{E}(c, Q) := \{c + Q^{\frac{1}{2}}x \mid x \in \mathbb{R}^n, x^\top x \leq 1\}$ , with center  $c \in \mathbb{R}^n$ . The Euclidean norm weighted by  $Q$  is denoted as  $\|x\|_Q = \sqrt{x^\top Q x}$ . Via the cyclic property of the trace operator  $\text{tr}(\cdot)$ , the trace trick allows the reformulation

$$x^\top Q x = \text{tr}(x^\top Q x) = \text{tr}(Q x x^\top). \quad (2)$$

## II. LINEARIZATION-BASED ELLIPSOIDAL TUBE OCP

We now derive a problem of structure (1) for the case of ellipsoidal uncertainty sets, which are propagated based on a linearization along the nominal trajectory [11], [16], [17]. A linear state feedback law is used to counteract tube growth. Consider the uncertain nonlinear dynamics

$$\tilde{x}_0 = \bar{x}_0, \quad \tilde{x}_{k+1} = \tilde{f}_k(\tilde{x}_k, \tilde{u}_k, w_k), \quad k = 0, \dots, N-1, \quad (3)$$

with uncertain state  $\tilde{x}_k \in \mathbb{R}^{n_x}$ , control  $\tilde{u}_k \in \mathbb{R}^{n_u}$  and perturbation  $w_k \in \mathbb{R}^{n_w}$ . We assume that the perturbation trajectory jointly lies inside an ellipsoidal set,  $w = (w_0, \dots, w_{N-1}) \in \mathcal{E}(0, W)$ , with  $W = \text{blkdiag}(W_0, \dots, W_{N-1})$ .

We describe the resulting uncertainty of the state trajectory by ellipsoidal tubes  $\mathcal{E}(x_k, P_k)$ , with  $P_k \in \mathbb{S}_+^{n_x}$ . Propagating the system for  $w_k = 0$  yields the nominal trajectory,

$$x_0 = \bar{x}_0, \quad x_{k+1} = \tilde{f}_k(x_k, u_k, 0), \quad k = 0, \dots, N-1. \quad (4)$$

The linear state feedback law

$$\tilde{u}_k = u_k + K_k(\tilde{x}_k - x_k), \quad \text{with } K_k \in \mathbb{R}^{n_u \times n_x}, \quad (5)$$

is used to counteract tube growth by reacting to deviations from the nominal trajectory. Based on a linearization at the nominal trajectory, we obtain the ellipsoid dynamics as

$$P_{k+1} = (A_k + B_k K_k) P_k (A_k + B_k K_k)^\top + \overbrace{\Gamma_k W_k \Gamma_k^\top}^{=: \tilde{W}_k} \quad (6)$$

$$=: \psi_k(x_k, u_k, P_k, K_k),$$

where the sensitivity matrices  $A_k$ ,  $B_k$ ,  $\Gamma_k$  depend on the nominal trajectory as

$$A_k = \nabla_x f_k(x_k, u_k, 0)^\top, \quad B_k = \nabla_u f_k(x_k, u_k, 0)^\top, \quad (7)$$

$$\Gamma_k = \nabla_w f_k(x_k, u_k, 0)^\top, \quad k = 0, \dots, N-1.$$

Given the ellipsoidal tube  $\tilde{x}_k \in \mathcal{E}(x_k, P_k)$ , linear state feedback (5), and a linearization of the constraint functions  $h_k^i(\tilde{x}_k, \tilde{u}_k)$  at the nominal trajectory, the backoffs in the robustified constraints (1e), (1f) can be obtained as the worst-case deviation from the nominal constraint value,

$$b_k^i(x_k, u_k, P_k, K_k) = \left\| \nabla_x h_k^i(x_k, u_k) + K_k^\top \nabla_u h_k^i(x_k, u_k) \right\|_{P_k}, \quad (8a)$$

$$b_N^i(x_N, P_N) = \left\| \nabla_x h_N^i(x_N) \right\|_{P_N}, \quad (8b)$$

for  $i = 1, \dots, n_h$ ,  $k = 0, \dots, N-1$ .

**Remark 1** (Linearization with respect to uncertainty). Under the given assumptions on  $w$ , the ellipsoid dynamics (6) and constraint robustification (8) are exact for linear dynamics  $f_k$  and constraints  $h_k$ , but otherwise subject to a linearization error. This error could be accounted for by adding additional terms in (6) resp. (8), cf., e.g., [13], [19], [20], [25].

**Remark 2** (Complexity of the standard OCP structure). Tube OCP (1) has a standard OCP sparsity structure with respect to the augmented state  $\check{x}_k = (x_k, \text{vec}(P_k))$  and augmented control  $\check{u}_k = (u_k, \text{vec}(K_k))$ . If  $P_k$ ,  $K_k$  parametrize an ellipsoidal tube under linear state feedback, the augmented state and control have dimensions  $\check{n}_x = n_x + \frac{1}{2}(n_x + n_x^2)$  and  $\check{n}_u = n_u + n_x n_u$ , where for  $\text{vec}(P_k)$  the symmetry of  $P_k$  is exploited. When solving (1) with a standard OCP algorithm, the computational complexity is  $\mathcal{O}((\check{n}_x^3 + \check{n}_x^2 \check{n}_u + \check{n}_x \check{n}_u^2 + \check{n}_u^3)N)$  per iteration [1]. With respect to the original state and control dimension, this corresponds to  $\mathcal{O}((n_x^6 + n_x^5 n_u + n_x^4 n_u^2 + n_x^3 n_u^3)N)$ .

**Remark 3** (Stochastic interpretation). In this section, we derived an OCP of structure (1) under the assumption of a set-based bound on the perturbation trajectory. The same OCP can be derived in a stochastic setting, for independent noise  $w_k$  with zero mean and covariance  $W_k$ . In this case,  $x_k$ ,  $P_k$  parametrize a distribution in state space with mean  $x_k$  and covariance  $P_k$ . The constraints (1e), (1f) are chance constraints, with the backoffs  $b_k^i$  corresponding to the standard deviation in constraint direction. In order to achieve a desired level of constraint satisfaction probability, the backoff needs to be multiplied by a corresponding factor [36].

### III. LINEAR QUADRATIC REGULATOR IN TUBE SPACE

A central building block of the presented algorithm is the update of the feedback gains and ellipsoidal tube for a given nominal trajectory.

Recall that  $P_k$  describes the deviations from the nominal trajectory as an ellipsoidal set,  $\tilde{x}_k - x_k \in \mathcal{E}(0, P_k)$ . Linear feedback on these deviations (5) induces a joint ellipsoid in the combined state-control space:

$$\begin{bmatrix} \tilde{x}_k - x_k \\ \tilde{u}_k - u_k \end{bmatrix} \in \mathcal{E}\left(0, \begin{bmatrix} P_k & P_k K_k^\top \\ K_k P_k & K_k P_k K_k^\top \end{bmatrix}\right). \quad (9)$$

We can optimize the trajectory of this ellipsoid, balancing uncertainty in different directions, by minimizing its weighted trace,

$$\min_{K, P} \sum_{k=0}^{N-1} \text{tr} \left( \overbrace{\begin{bmatrix} Q_k & S_k^\top \\ S_k & R_k \end{bmatrix}}^{C_k} \overbrace{\begin{bmatrix} P_k & P_k K_k^\top \\ K_k P_k & K_k P_k K_k^\top \end{bmatrix}}^{\tilde{P}_k} \right) + \text{tr}(Q_N P_N) \quad (10a)$$

$$\text{s.t.} \quad P_0 = \tilde{P}_0, \quad (10b)$$

$$P_{k+1} = (A_k + B_k K_k) P_k (A_k + B_k K_k)^\top + \tilde{W}_k, \quad k = 0, \dots, N-1. \quad (10c)$$

This is an OCP in ellipsoidal tube space with state  $P_k$  and control  $K_k$ . In order to interpret the objective, we note that the trace of a positive semidefinite matrix is given by the sum of its eigenvalues, which in turn are the squared axis lengths of the corresponding ellipsoid. In this sense, (10) minimizes squared deviations in the state-control space, weighted by  $C_k$ , such that we also refer to  $C_k$  as a ‘‘Hessian’’.

In fact, (10) can alternatively be derived as a reformulation of the standard stochastic LQR problem, cf. [11]. In this context,  $P_k$  and  $\tilde{P}_k$  are covariance matrices, and (10) minimizes the expected value of the squared deviation. This follows from

$$\begin{aligned} & \mathbb{E}_{\tilde{z}_k} \{ (\tilde{z}_k - z_k)^\top C_k (\tilde{z}_k - z_k) \} \\ &= \mathbb{E}_{\tilde{z}_k} \{ \text{tr} (C_k (\tilde{z}_k - z_k) (\tilde{z}_k - z_k)^\top) \} = \text{tr}(C_k \tilde{P}_k), \end{aligned} \quad (11)$$

where we used  $\tilde{z}_k = (\tilde{x}_k, \tilde{u}_k)$  for the uncertain state-control trajectory with mean  $z_k$  and covariance  $\tilde{P}_k$ , and the second line follows from the trace trick (2).

As a classical result, for the stochastic LQR, the optimal feedback gains are given by a Riccati recursion, which due to certainty equivalence is independent of the noise contribution  $\tilde{W}$  [37]. This holds true for the algebraic structure of (10) in general, independent of the interpretation of  $P_k$  as covariances or ellipsoidal sets.

**Lemma 1** ([11]). *Let  $Q_N \succeq 0$ ,  $C_k \succeq 0$ ,  $Q_k \succeq 0$ ,  $R_k \succ 0$ , for  $k = 0, \dots, N-1$ . Further, let  $P_k \succ 0$  for all  $P_k$  reachable with dynamics (10c),  $k = 0, \dots, N$ . Then, the solution to (10) is uniquely defined by the backward Riccati recursion*

$$V_N = Q_N, \quad (12a)$$

$$K_k^* = -(R_k + B_k^\top V_{k+1} B_k)^{-1} (S_k + B_k^\top V_{k+1} A_k), \quad (12b)$$

$$V_k = Q_k + A_k^\top V_{k+1} A_k + (S_k^\top + A_k^\top V_{k+1} B_k) K_k^*, \quad (12c)$$

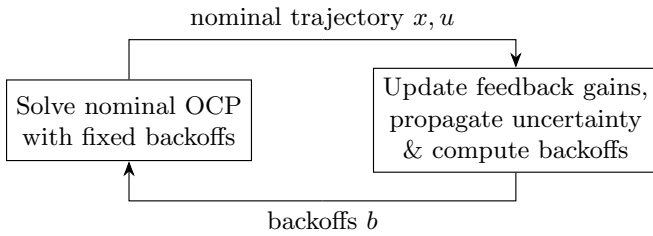


Fig. 1. Schematic structure of Riccati-ZORO

for  $k = N - 1, \dots, 0$ , followed, for  $k = 0, \dots, N - 1$ , by the forward Lyapunov recursion

$$P_0^* = \bar{P}_0, \quad (13a)$$

$$P_{k+1}^* = (A_k + B_k K_k^*) P_k^* (A_k + B_k K_k^*)^\top + \tilde{W}_k. \quad (13b)$$

#### IV. RICCATI-ZORO

In this section we describe the algorithm Riccati-ZORO, which is aimed at problems of structure (1), but optimizes the feedback gains based on a heuristic cost instead of exactly. We consider two choices for the heuristic cost, and discuss the relation to the algorithms ZORO and SIRO.

##### A. Structure of the algorithm

Riccati-ZORO alternates between solving a nominal OCP with fixed backoffs  $b$ , and a feedback gain optimization problem for a fixed nominal trajectory, which subsequently yields updated backoffs. This structure is visualized in Fig 1.

1) *Nominal OCP with fixed backoffs*: By computing the backoffs for fixed values of  $P$  and  $K$  in (1), we obtain the first subproblem as

$$\min_{x, u} \sum_{k=0}^{N-1} l_k(x_k, u_k) + l_N(x_N) \quad (14a)$$

$$\text{s.t.} \quad x_0 = \bar{x}_0, \quad (14b)$$

$$x_{k+1} = f_k(x_k, u_k), \quad k = 0, \dots, N - 1, \quad (14c)$$

$$0 \geq h_k(x_k, u_k) + b_k, \quad k = 0, \dots, N - 1, \quad (14d)$$

$$0 \geq h_N(x_N) + b_N, \quad (14e)$$

which has the structure of a standard nominal OCP.

The solution of (14) yields an updated nominal trajectory. The second subproblem, described below, optimizes the feedback gains for this updated trajectory by solving (10). From the resulting tube, updated backoffs are computed, cf. Fig. 1.

Treating the backoffs as fixed neglects their dependence on the tube variables, which depend on the nominal trajectory. Since this disregards first-order derivatives, the resulting algorithm is a zero-order method, as discussed in Section V.

For intermediate iterations of Riccati-ZORO, subproblem (14) can be infeasible due to large backoffs, even if (1) is feasible. In this case, one can enforce the inequality constraint via an exact penalty on constraint violation, instead of explicit hard constraints [38]. This yields an exact solution of (14) if feasible, and otherwise minimizes constraint violation.

For simplicity of presentation, we assume that in each iteration, (14) is solved up to convergence. Alternatively, one

---

#### Algorithm 1 Riccati-ZORO

---

**Input:** Initial guess  $x, u$  (e.g. solution to nominal OCP)  
**while** not\_converged **do**  
 $K \leftarrow \text{riccati\_recursion}(x, u)$  // (12)  
 $P \leftarrow \text{propagate\_ellipsoids}(x, u, K)$  // (13)  
 $b \leftarrow \text{compute\_backoffs}(x, u, P, K)$  // (8)  
 $x, u \leftarrow \text{solve\_perturbed\_ocp}(b)$  // (14)  
**return:**  $x, u, P, K$

---

can update the backoffs already earlier, e.g., after performing a single SQP iteration on (14), thereby avoiding unnecessary iterations on a problem that is ultimately not of interest. This is discussed in more detail in Section VI.

2) *Tube optimization via Riccati recursion*: In the second subproblem, the feedback gains are updated for the current nominal trajectory. This is achieved by solving (10), which optimizes the trajectory of the joint state-control ellipsoid by minimizing its size, using the weighted trace as metric. Crucially, we allow the weighting matrix  $C_k$  to depend on the nominal trajectory. By Lemma 1, the solution of (10) is given by a Riccati recursion followed by the ellipsoid propagation. Overall, the computational steps of Riccati-ZORO are given in Algorithm 1.

##### B. Uncertainty cost design

We consider two choices for the uncertainty weighting matrices  $C_k$  used in the tube optimization subproblem (10).

1) *Trajectory-independent weighting*: The most straightforward choice is to update the feedback gains by solving (10) with cost matrices independent of the nominal trajectory, as proposed in [13]. This provides a trajectory-independent balancing of uncertainty across all directions of the state-control space, but does not systematically trade off uncertainties between directions according to their performance impact. For the tuning of this cost, the same intuitions as for standard LQR hold.

2) *Constraint-adaptive weighting*: Here, we derive a weighting scheme that prioritizes reduction of the uncertainty in constraint direction, yielding smaller backoffs, based on the proximity of the nominal trajectory to the constraint. This weighting is most intuitively derived through the approximate expected value of a logarithmic barrier function, though as a heuristic, it remains independent of the specific interpretation of the ellipsoids.

First, consider a nonlinear cost function  $\hat{l}_k(\tilde{z}_k)$ . Given uncertain  $\tilde{z}_k$  with mean  $z_k$  and covariance  $\tilde{P}_k$ , we can approximate its expectation via a second-order Taylor expansion as

$$\begin{aligned} \mathbb{E}_{\tilde{z}_k} \{\hat{l}_k(z_k)\} &\approx \mathbb{E}_{\tilde{z}_k} \left\{ \hat{l}_k(z_k) + \nabla \hat{l}_k(z_k)^\top (\tilde{z}_k - z_k) \right. \\ &\quad \left. + \frac{1}{2} (\tilde{z}_k - z_k)^\top \nabla^2 \hat{l}_k(z_k) (\tilde{z}_k - z_k) \right\} \quad (15) \\ &= \hat{l}_k(z_k) + \frac{1}{2} \text{tr}(\nabla^2 \hat{l}_k(z_k) \tilde{P}_k), \end{aligned}$$

where the second-order term follows from (11). The first term is the nominal cost, whereas the second term penalizes covariance weighted by the nominal curvature.

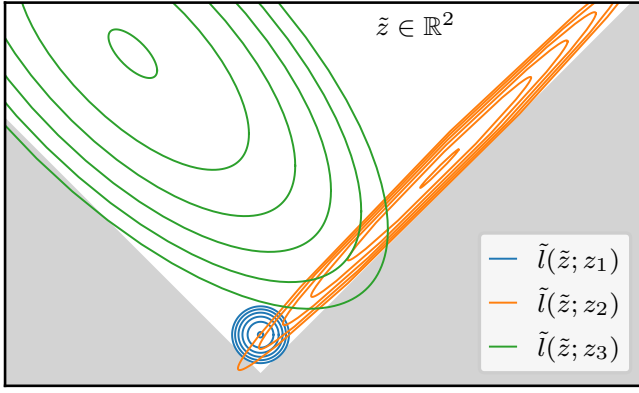


Fig. 2. Visualization of the constraint-adaptive uncertainty weighting  $C(z)$  in (17), for  $z \in \mathbb{R}^2$ , and with  $\bar{C} = 0$  and  $\tau = 1$ . The figure shows the contour lines of the quadratic uncertainty penalization  $\tilde{l}(\tilde{z}; z) = (\tilde{z} - z)^\top C(z)(\tilde{z} - z)$  for the three exemplary values  $z_1, z_2, z_3$ . The gray area is the infeasible region. As  $z$  approaches the boundaries of the feasible set, the penalty becomes steeper for the corresponding constraint direction.

Now, consider enforcing the inequality  $h_k^i(\tilde{z}_k) \leq 0$  with  $\tilde{z}_k = (\tilde{x}_k, \tilde{u}_k)$  via a log-barrier term  $\tilde{l}_k^i(\tilde{z}_k) = \tau_k^i \phi(h_k^i(\tilde{z}_k))$ , with logarithmic barrier function  $\phi(\eta) = -\log(-\eta)$  weighted by  $\tau_k^i > 0$ . We approximate its expectation based on (15), using the approximate Hessian

$$\nabla^2 \tilde{l}_k^i(z_k) \approx \tau_k^i \nabla h_k^i(z_k) \phi''(h_k^i(z_k)) \nabla h_k^i(z_k)^\top \succeq 0, \quad (16)$$

which results from an additional linearization of the constraint function. Since here we are only interested in deriving a heuristic cost on uncertainty, we drop the nominal term in (15). Adding an additional regularization term  $\bar{C}_k \succeq 0$  yields an objective of structure (10a) with cost matrices

$$C_k(z_k) = \bar{C}_k + \sum_{i=0}^{n_{h_k}} \tau_k^i \phi''(h_k^i(z_k)) \nabla h_k^i(z_k) \nabla h_k^i(z_k)^\top. \quad (17)$$

The terms inside the sum correspond to the squared backoff terms penalized by the barrier curvature, as can be seen via the backoff definition (8) and trace trick (2). This smoothly increases the penalty on a backoff term as the nominal trajectory approaches the corresponding constraint boundary. The corresponding quadratic cost on deviations from the nominal trajectory, cf. (11), is visualized in Fig. 2.

By adapting the weights  $\tau_k^i$ , uncertainty can be traded off across different constraints. A small trajectory-independent term  $\bar{C}_k$  can serve as a baseline.

As a heuristic, the performance of Riccati-ZORO depends on the uncertainty cost design. If a good approximation of the optimal solution of (1) can be achieved by keeping all backoffs small, Riccati-ZORO is expected to perform well with minor tuning effort. However, if performance is highly sensitive to accurately capturing the optimal balance between backoffs, closely approximating the optimal solution of (1) via Riccati-ZORO may require significant tuning effort.

### C. Computational complexity

Solving the nominal OCP (14) with standard OCP algorithms incurs a computational cost of  $\mathcal{O}((n_x^3 + n_x^2 n_u + n_x n_u^2 + n_u^3)N)$

[1]. The Riccati recursion (12) has the same complexity, and the Lyapunov recursion (13) has  $\mathcal{O}((n_x^3 + n_x^2 n_u)N)$ . Thus, the overall complexity of Riccati-ZORO is  $\mathcal{O}((n_x^3 + n_x^2 n_u + n_x n_u^2 + n_u^3)N)$  per iteration, which is the same complexity as a nominal OCP. In contrast, solving (1) directly with standard OCP solvers incurs a cost of  $\mathcal{O}((n_x^6 + n_x^5 n_u + n_x^3 n_u^2 + n_x^3 n_u^3)N)$ , cf. Remark 2.

### D. Relation to ZORO and SIRO

Both ZORO and SIRO are closely related to Riccati-ZORO. ZORO targets a simplified version of (1), in which the feedback gains  $K$  are set to a prechosen value  $\bar{K}$  [26], [29]. Thus, in each iteration it only updates the ellipsoid propagation and the backoffs. In this sense, Riccati-ZORO generalizes ZORO. In both variants, the backoff values are essentially functions of the nominal trajectory only, since the tube parameters could in principle be eliminated. Thus, on a high level, they address an identical problem structure, such that the theoretical properties of ZORO [26] can be generalized to Riccati-ZORO, as discussed in Section V.

SIRO addresses the full problem (1) for the case that the uncertainty dynamics and backoffs are given in the form (6) and (8). Like Riccati-ZORO, it updates the feedback parameters by solving a problem of structure (10) in each iteration. Crucially, in SIRO the cost matrices for this update are not chosen heuristically, but derived from the optimality conditions of (1). This results in the cost matrices

$$C_k(z_k, \mu_k) = \bar{C}_k + \sum_{i=0}^{n_{h_k}} \frac{\mu_k^i}{2b_k^i} \nabla h_k^i(z_k) \nabla h_k^i(z_k)^\top, \quad (18)$$

with  $\mu_k^i$  the Lagrange multiplier of the constraint  $h_k^i$  in (14). This informs the tube optimization problem (10) exactly on the cost of each backoff. However, the dependence of (18) on the multipliers  $\mu_k^i$  can create an algorithmic instability, keeping SIRO from converging. This relates to active set changes of (14), which cause a nonsmooth change in the value of  $\mu_k^i$ . Given the structural similarity, the barrier Hessian in (17) can be understood as a heuristic smoothing of the exact cost (18). As a minor difference, SIRO as presented in [11] uses a gradient correction and is therefore not a zero-order method.

### V. ANALYSIS OF OPTIMALITY AND CONVERGENCE

In this section, we analyze the points to which Riccati-ZORO converges. In comparison to the exact feedback gain optimization problem (1), we introduced two sources of suboptimality with respect to the cost function. The first results from the heuristic choice of feedback gains, while the second is a consequence of the zero-order backoff updates. In both cases, constraint satisfaction and any associated guarantees remain uncompromised.

We start by writing (1) on a more abstract level. By eliminating the nominal and uncertainty state trajectories  $x$  and  $P$  based on their dynamics (1c), (1d), and correspondingly redefining the objective and inequality constraints, we obtain

$$\min_{u, K} f(u) \quad \text{s.t.} \quad h(u) + \sigma b(\bar{u}, K) \leq 0 \quad (19)$$

as the sequential formulation of (1). We additionally introduce the parameter  $\sigma > 0$  as the level of uncertainty. This corresponds to substituting  $\sigma^2 \bar{P}_0$  in (1b) and  $\sigma^2 \bar{W}_k$  in (6). In Riccati-ZORO, instead of solving (19) exactly, the feedback gains  $K$  are heuristically chosen as the solution of an optimization problem parametrized by  $u$ ,

$$\tilde{K}(u) = \arg \min_K F(u, K), \quad (20)$$

which in our case is given by (10). This heuristic choice of feedback gains corresponds to a restriction of (19) to

$$\min_u f(u) \quad \text{s.t.} \quad h(u) + \sigma b(u, \tilde{K}(u)) \leq 0, \quad (21)$$

where the nominal trajectory remains as the only degree of freedom. In general, a heuristic choice of  $\tilde{K}(u)$  will not account exactly for the implicit cost of the backoffs, such that solving (21) yields a suboptimal solution of (19).

When iteratively solving (21) for fixed backoffs, the backoff gradient is neglected. This corresponds to a zero-order approximation of the constraint gradient [26]. In consequence, stationary points  $\hat{u}$  of Riccati-ZORO are not exact solutions of (21). Instead, they are solutions of a perturbed version of (21), given by

$$\min_u f(u) + \sigma \hat{c}^\top u \quad \text{s.t.} \quad h(u) + \sigma b(u, \tilde{K}(u)) \leq 0, \quad (22)$$

with gradient perturbation  $\hat{c} = \frac{d}{du} b(\hat{u}, \tilde{K}(\hat{u}))^\top \hat{\mu}$  resulting from the neglected backoff gradient evaluated at the stationary point  $\hat{u}$  with Lagrange multiplier  $\hat{\mu}$ . Note that this perturbation only modifies the objective function. The constraints satisfaction remains unaffected.

For more detail, we refer to [26], which analyzes the corresponding suboptimality for ZORO and proves local convergence of ZORO for sufficiently small  $\sigma$ . ZORO addresses (21) for the special case of a constant feedback gain,  $\tilde{K}(u) \equiv \bar{K}$ . Thus, the only difference is that Riccati-ZORO additionally neglects the gradient of  $\tilde{K}(u)$ , such that the core arguments of the proofs in [26] also apply to Riccati-ZORO. In [27], optimality is recovered via a gradient correction, which in our case would need derivatives of the Riccati recursion and ellipsoid propagation.

## VI. EFFICIENT IMPLEMENTATION IN acados

We provide an efficient open-source implementation of Riccati-ZORO in acados [28] by extending the ZORO implementation described in [29]. The implementation is written in C, using BLASFEO [39] for the linear algebra, and accessible via the acados Python and Matlab interfaces. The robust OCP can be conveniently defined on top of a standard acados OCP by specifying the uncertainty-related quantities. Additionally, the online adaptation of externally computed covariance matrices, as needed for example in GP-MPC [31], is supported via the extension in [32].

The solution of a nominal OCP via an SQP method requires at each time step the computation of the sensitivities of the dynamics and constraints, which is typically a major part of the computational load. These are the same sensitivities used

in the Riccati recursion (12), ellipsoid propagation (13) and backoff computation (8).

The acados custom update functionality introduced in [29] allows for the execution of a custom C function in between the OCP solver calls, which can access and modify the solver data. Riccati-ZORO extends the ZORO custom update. Overall, with each call it: (i) accesses the dynamic and constraint sensitivities, which have already been computed as part of the OCP solver call, (ii) uses BLASFEO to perform the backoff update including Riccati recursion, ellipsoid propagation, and backoff computation, and (iii) updates the inequality constraint bounds with the new backoffs.

This implementation is released in <https://github.com/acados/acados/releases/tag/v0.5.2>.

## VII. NUMERICAL EXPERIMENTS

In this section, we compare Riccati-ZORO to exact feedback optimization, based on an implementation in CasADi [35] with IPOPT [40] as solver, followed by a benchmark of the computational performance of the acados implementation, and a case study from industrial research. All experiments are performed on a standard Laptop with an Intel i7-8565U CPU and 16 GB of RAM. The code is available at <https://github.com/fmesserer/riccati-zoro>.

### A. Towing Kite (with CasADi & IPOPT)

We use the towing kite example from [11] to compare the two Riccati-ZORO variants to the optimal solution of (1). The towing kite is connected to a ship via a tether of constant length and the objective is to maximize the average thrusting force in order to tow the ship, while respecting a minimum height constraint. The kite position is described by the angles  $\theta$  and  $\phi$  and its orientation by the angle  $\psi$ , resulting in the state  $x = (\phi, \theta, \psi)$ , with the steering deflection  $u \in \mathbb{R}$  as control input. The main source of uncertainty is the unknown wind speed. For more details, see [11]. Due to its nonlinear economic objective function and highly nonlinear dynamics, this is a very challenging problem.

We compare the fixed and constraint-adaptive variants of Riccati-ZORO to the exact solution obtained with SIRO and the solution obtained by ZORO with fixed feedback  $K = 0$ . For the constant Hessian variant of Riccati-ZORO, we use  $Q_k = I$ ,  $R_k = 10^{-2}$ . The results are shown in Fig. 3.

With the feedback gains computed based on a constant Hessian, Riccati-ZORO is able to achieve a balanced reduction of uncertainty in all direction. In contrast, using the adaptive Hessian reduces uncertainty specifically in constraint direction, such that for this example there is effectively no suboptimality with respect to exact feedback gain optimization. For a rough comparison of timings, we initialize all solvers at the nominal trajectory. ZORO, both Riccati-ZORO variants, and SIRO all need 6 or 7 iterations and  $0.45 \pm 0.05$  s to converge. In comparison, when solving (1) directly, IPOPT needs 16.3 s for the problem with fixed feedback gains  $K = 0$ , and does not converge for the full feedback gain optimization problem.

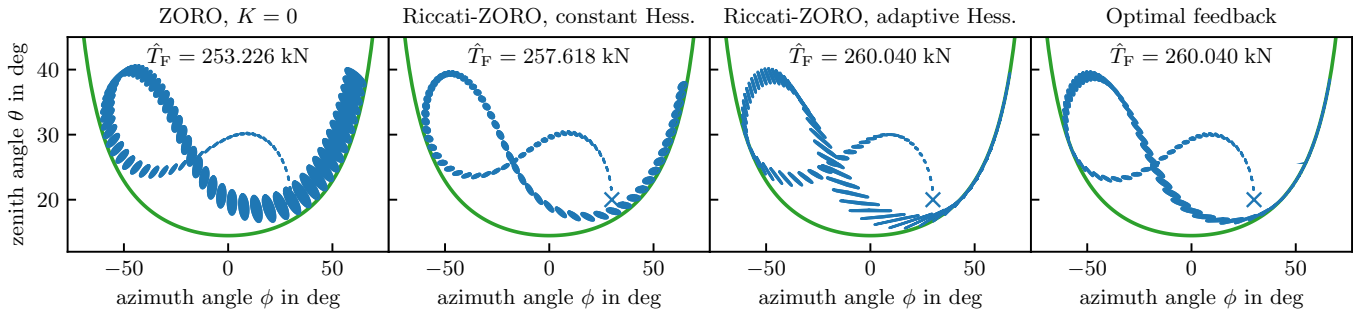


Fig. 3. Stationary points of different algorithms for the towing kite problem, with the objective of maximizing the average thrusting force  $\hat{T}_F$ . In comparison, the exact solution of the fixed feedback problem with  $K = 0$  with  $\hat{T}_F = 253.235$  kN looks indistinguishable from the ZORO solution. The nominal problem with zero backoff has  $\hat{T}_F = 260.086$  kN.

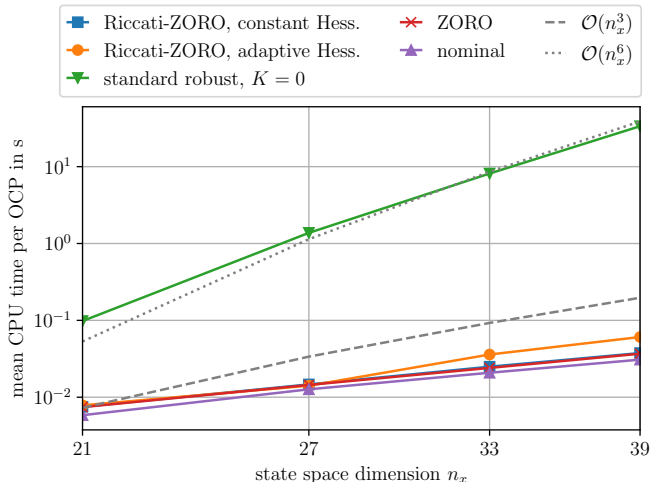


Fig. 4. Computation times for the hanging chain of masses benchmark.

### B. Hanging chain of masses (with acados)

In order to investigate the complexity with respect to the state dimension, we use the hanging chain of masses benchmark in the setting detailed in [29]. By changing the number of masses in the chain, this example allows for a flexible scaling of the state space dimension  $n_x$ . We compare the acados implementation of the two variants of Riccati-ZORO to nominal MPC and ZORO with fixed feedback  $K = 0$ . As a reference, we formulate and solve the robust OCP with fixed feedback  $K = 0$  as a standard OCP with augmented state. This serves as a loose lower bound on the computational time for the more challenging OCP with feedback optimization. For each variant, we perform five closed-loop MPC simulations of 40 timesteps each, and average over the resulting computation times. Each MPC solver is fully converged for every time step. The results are shown in Fig. 4. The Riccati recursion adds only very little computational cost in comparison with the nominal OCP and ZORO. Due to the added nonlinearity from the trajectory-dependent uncertainty weighting, the constraint-adaptive Riccati-ZORO variant needs slightly more iterations than ZORO and Riccati-ZORO with a constant Hessian.

### C. Collision avoidance (with acados)

As a practical case study, we consider collision avoidance MPC for a differential drive robot. This problem formulation has previously been employed for the real-world application of ZORO-MPC in [30]. For this problem, SIRO exhibits unreliable convergence depending on the specific instances of (1) encountered throughout the MPC loop.

The dynamic model uses the state  $x = (p_x, p_y, \theta, v, \omega)$ , consisting of positions  $(p_x, p_y)$ , orientation  $\theta$ , speed  $v$ , and angular velocity  $\omega$ . The controls are the acceleration  $a$  and angular acceleration  $\alpha$ . The robot should track a given reference trajectory while avoiding collision and respecting constraints on the speed, angular velocity, and actuator limits. For more details, see [29], [30].

We compare two MPC policies: (i) ZORO with a constant feedback gain, which has been designed ad-hoc specifically for the differential drive robot [30], (ii) Riccati-ZORO with an adaptive Hessian. For each MPC policy we use the RTI variant, with two SQP iterations per time step, and a prediction horizon of  $N = 20$ . The results are shown in Fig. 5.

The online optimization of the feedback gains enables improved reference tracking in the vicinity of obstacles, while the computational cost is only marginally increased by the Riccati recursion. Furthermore, note that some design effort went into the application-specific feedback gain design, while the Riccati-ZORO approach is generic. For nonlinear systems in general, no predesigned feedback gain is available.

## VIII. CONCLUSION

We have presented the algorithm Riccati-ZORO for heuristic feedback gain optimization in tube-based robust and stochastic MPC. While the key principle is relevant to a variety of nonlinear tube OCPs, we have developed it specifically to the case of ellipsoidal tubes with linearization based dynamics. Future work should extend it to a broader range of formulations. Of specific interest are tube OCPs that provide robustness guarantees for the nonlinear case, and those using a learning-based uncertainty quantification. Furthermore, due to its close connection to SIRO, the heuristic multiplier smoothing could serve as a basis towards exact feedback gain optimization with broader convergence guarantees.

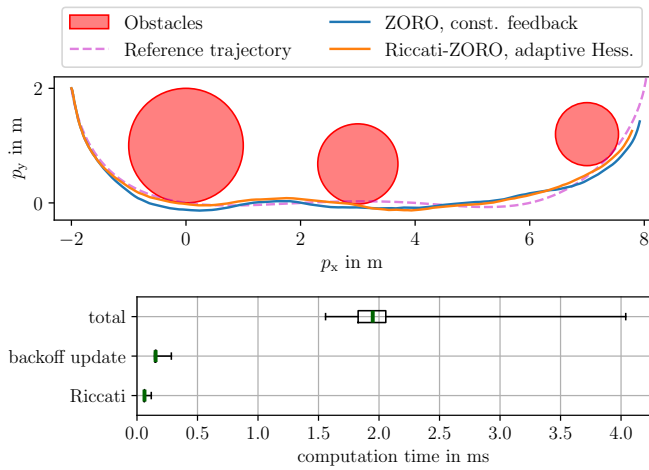


Fig. 5. Top: Closed-loop trajectories for the differential drive collision avoidance case study. The online feedback optimization of Riccati-ZORO enables closer tracking of the reference in the vicinity of obstacles, resulting in a minimum obstacle distance of 0.009 m, compared to 0.058 m for ZORO with precomputed feedback.

Bottom: Computational cost per MPC step for Riccati-ZORO. The total time includes the nominal SQP step and the backoff update. The backoff update includes the Riccati recursion, the ellipsoid propagation, and the backoff computation given the ellipsoids. The added computational cost in comparison with the nominal OCP is only a fraction of the latter.

## REFERENCES

- [1] J. B. Rawlings, D. Q. Mayne, and M. M. Diehl, *Model Predictive Control: Theory, Computation, and Design*, 2nd ed. Nob Hill, 2017.
- [2] B. Kouvaritakis and M. Cannon, *Model Predictive Control. Classical, Robust and Stochastic*. Springer, 2016.
- [3] P. O. M. Scokaert and D. Q. Mayne, "Min-max feedback model predictive control for constrained linear systems," *IEEE Trans. Automatic Control*, vol. 43, pp. 1136–1142, 1998.
- [4] G. C. Calafiore and M. C. Campi, "The scenario approach to robust control design," *IEEE Trans. Automat. Control*, 2006.
- [5] S. Lucia, J. A. E. Andersson, H. Brandt, M. Diehl, and S. Engell, "Handling uncertainty in economic nonlinear model predictive control: A comparative case study," *J. Process Control*, vol. 24, 2014.
- [6] W. Langson, S. R. I. Chrysochoos, and D. Q. Mayne, "Robust model predictive control using tubes," *Automatica*, vol. 40, no. 1, 2004.
- [7] D. Mayne, E. Kerrigan, E. J. van Wyk, and P. Falugi, "Tube-based robust nonlinear model predictive control," *International Journal of Robust and Nonlinear Control*, vol. 21, pp. 1341–1353, 2011.
- [8] S. V. Raković, *Robust Model Predictive Control*. London: Springer, 2019, pp. 1–11.
- [9] J. Köhler, P. Kötting, R. Soloperto, F. Allgöwer, and M. A. Müller, "A robust adaptive model predictive control framework for nonlinear uncertain systems," *International Journal of Robust and Nonlinear Control*, vol. 31, no. 18, pp. 8725–8749, 2021.
- [10] Z. Nagy and R. Braatz, "Open-loop and closed-loop robust optimal control of batch processes using distributional and worst-case analysis," *Journal of Process Control*, vol. 14, pp. 411–422, 2004.
- [11] F. Messerer and M. Diehl, "An efficient algorithm for tube-based robust nonlinear optimal control with optimal linear feedback," in *Proc. IEEE Conf. Decis. Control (CDC)*, 2021.
- [12] A. P. Leeman, J. Sieber, S. Bennani, and M. N. Zeilinger, "Robust optimal control for nonlinear systems with parametric uncertainties via system level synthesis," *Proc. IEEE Conf. Decis. Control (CDC)*, 2023.
- [13] D. D. Leister and J. P. Koeln, "Robust model predictive control for nonlinear discrete-time systems using iterative time-varying constraint tightening," *Proc. Amer. Control Conf. (ACC)*, 2025.
- [14] T. Belvedere, M. Cognetti, G. Oriolo, and P. R. Giordano, "Sensitivity-aware model predictive control for robots with parametric uncertainty," *IEEE Transactions on Robotics*, vol. 41, 2025.
- [15] S. Zhang and J. Swevers, "Robustified time-optimal point-to-point motion planning and control under uncertainty," *Eur. J. Control*, 2025.
- [16] M. Diehl, H. Bock, and E. Kostina, "An approximation technique for robust nonlinear optimization," *Math. Program.*, vol. 107, 2006.
- [17] B. Houska and M. Diehl, "Robustness and stability optimization of power generating kite systems in a periodic pumping mode," in *Proc. IEEE Multi-Conf. Systems and Control (MSC)*, Yokohama, Japan, 2010.
- [18] T. Koller, F. Berkenkamp, M. Turchetta, and A. Krause, "Learning-based model predictive control for safe exploration," in *Proc. IEEE Conf. Decis. Control (CDC)*, 2018, pp. 6059–6066.
- [19] B. Houska, "Robust optimization of dynamic systems," Ph.D. dissertation, KU Leuven, 2011.
- [20] T. Kim, P. Elango, and B. Açıkmeşe, "Joint synthesis of trajectory and controlled invariant funnel for discrete-time systems with locally lipschitz nonlinearities," *Int J Robust Nonlinear Control*, vol. 34, 2024.
- [21] L. Hewing, J. Kabzan, and M. N. Zeilinger, "Cautious model predictive control using gaussian process regression," *IEEE Transaction on Control Systems Technology*, vol. 28, no. 6, pp. 2736–2743, 2020.
- [22] M. Farina, L. Giulioni, L. Magni, and R. Scattolini, "An approach to output-feedback MPC of stochastic linear discrete-time systems," *Automatica*, vol. 55, pp. 140–149, 2015.
- [23] F. Messerer, K. Baumgärtner, and M. Diehl, "A dual-control effect preserving formulation for nonlinear output-feedback stochastic model predictive control with constraints," *IEEE Contr. Syst. Lett.*, vol. 7, 2023.
- [24] P. J. Goulart, E. C. Kerrigan, and J. M. Maciejowski, "Optimization over state feedback policies for robust control with constraints," *Automatica*, vol. 42, pp. 523–533, 2006.
- [25] A. P. Leeman, J. Köhler, A. Zanelli, S. Bennani, and M. N. Zeilinger, "Robust nonlinear optimal control via system level synthesis," *IEEE TAC*, vol. 70, no. 7, 2025.
- [26] A. Zanelli, J. Frey, F. Messerer, and M. Diehl, "Zero-order robust nonlinear model predictive control with ellipsoidal uncertainty sets," *IFAC-PapersOnLine*, vol. 54, no. 6, 2021.
- [27] X. Feng, S. D. Cairano, and R. Quirynen, "Inexact Adjoint-based SQP Algorithm for Real-Time Stochastic nonlinear MPC," in *Proc. IFAC World Congr.*, 2020.
- [28] R. Verschuereen, G. Frison, D. Kouzoupis, J. Frey, N. van Duijkeren, A. Zanelli, B. Novoselnik, T. Albin, R. Quirynen, and M. Diehl, "acados – a modular open-source framework for fast embedded optimal control," *Math. Program. Comput.*, pp. 147–183, 2021.
- [29] J. Frey, Y. Gao, F. Messerer, A. Lahr, M. N. Zeilinger, and M. Diehl, "Efficient zero-order robust optimization for real-time model predictive control with acados," in *Proc. Eur. Control Conf. (ECC)*, 2024.
- [30] Y. Gao, F. Messerer, J. Frey, N. van Duijkeren, and M. Diehl, "Collision-free motion planning for mobile robots by zero-order robust optimization-based MPC," in *Proc. Eur. Control Conf. (ECC)*, 2023.
- [31] A. Lahr, A. Zanelli, A. Carron, and M. N. Zeilinger, "Zero-order optimization for Gaussian process-based model predictive control," *European Journal of Control*, vol. 74, p. 100862, 2023.
- [32] A. Lahr, J. Näf, K. P. Wabersich, J. Frey, P. Siehl, A. Carron, M. Diehl, and M. N. Zeilinger, "L4acados: Learning-based models for acados, applied to gaussian process-based predictive control," *IEEE Transactions on Control Systems Technology*, 2024.
- [33] S. Zhang, M. Bos, B. Vandewal, W. Decré, J. Gillis, and J. Swevers, "Robustified time-optimal collision-free motion planning for autonomous mobile robots under disturbance conditions," *IEEE International Conference on Robotics and Automation (ICRA)*, 2024.
- [34] A. P. Leeman, J. Köhler, F. Messerer, A. Lahr, M. Diehl, and M. N. Zeilinger, "Fast system level synthesis: Robust model predictive control using riccati recursions," *IFAC-PapersOnLine*, vol. 58, no. 18, 2024.
- [35] J. A. E. Andersson, J. Gillis, G. Horn, J. B. Rawlings, and M. Diehl, "CasADi – a software framework for nonlinear optimization and optimal control," *Math. Program. Comput.*, vol. 11, no. 1, pp. 1–36, 2019.
- [36] A. Mesbah, "Stochastic model predictive control: An overview and perspectives for future research," *IEEE Control Systems Magazine*, vol. 36, no. 6, pp. 30–44, 2016.
- [37] R. F. Stengel, *Optimal Control and Estimation*. Dover, 1986.
- [38] J. Nocedal and S. J. Wright, *Numerical Optimization*, 2nd ed., ser. Operations Research and Financial Eng. Springer-Verlag, 2006.
- [39] G. Frison, D. Kouzoupis, T. Sartor, A. Zanelli, and M. Diehl, "BLAS-FEO: Basic linear algebra subroutines for embedded optimization," *ACM Trans. Math. Softw.*, vol. 44, no. 4, pp. 42:1–42:30, 2018.
- [40] A. Wächter and L. T. Biegler, "On the implementation of an interior-point filter line-search algorithm for large-scale nonlinear programming," *Math. Program.*, vol. 106, no. 1, pp. 25–57, 2006.